Seismic Attributes for Fault/Fracture Characterization*

Satinder Chopra[1] and Kurt J. Marfurt[2]

Search and Discovery Article #41539 (2015)
Posted March 2, 2015

*Adapted from extended abstract prepared in conjunction with a presentation given at CSPG/CSEG 2007 GeoConvention, Calgary, AB, Canada, May 14-17, 2007, CSPG/CSEG/Datapages © 2015

[1]Arcis Corporation, Calgary, AB, Canada (schopra@arcis.com)
[2]University of Houston, Houston, TX, United States

Abstract

Among the various geophysical techniques available for characterizing faults and fractures, 3D seismic attributes have proven to be some of the most useful. One of the greatest strengths of 3D seismic is the dense, regular sampling of data over the region of interest, providing images that accurately represent the areal extent of the features. When seismic amplitude changes associated with the features of interest are not noticeable on vertical sections, horizontal time or horizon slices often yield distinctive patterns that are easily recognizable. Among the more valuable seismic attributes are those sensitive to reservoir impedance, thickness, or geomorphology. Although there are a few hundred seismic attributes that are in common use today, here we discuss the application of poststack attributes for the detection of faults and fractures. Dip-magnitude, dip-azimuth, and coherence attributes have been used for the detection of faults and fractures since the early to mid-1990s. We demonstrate the value of using these attributes as well as the more recently developed volumetric curvature attributes in the mapping of faults and fractures in the North Sea.

Discontinuity Attributes

Seismic attributes that highlight discontinuities in the seismic data are useful for fault and fracture characterization.

Dip-Magnitude and Dip-Azimuth

Rijks and Jaufred (1991) showed how maps of dip-magnitude and dip-azimuth computed from interpreted horizons can highlight faults with displacements having offsets significantly less than the width of the seismic wavelet.

Coherence

Bahorich and Farmer (1995), Marfurt et al. (1998), Marfurt et al. (1999), and Gerztenkorn and Marfurt (1999) developed coherence attributes which compared adjacent seismic waveforms using cross correlation, semblance, and eigen structure measures along the dip and azimuth of seismic reflector.

The coherence images clearly reveal buried deltas, river channels, reefs, and dewatering features. The remarkable detail with which stratigraphic features show up on coherence displays, with no interpretation bias and some previously unidentifiable even with close scrutiny, appeal to interpreters who do not have the time for a complete conventional interpretation but wish to place their prospects in the appropriate geologic context.

In Figure 1a and Figure 1b, we show a comparison of a seismic time slice (t = 1240 ms) with its equivalent coherence slice. The coherence volume was generated using a modified eigen decomposition algorithm, which employs a robust dip steering option for removal of the structural component (dip) from the coherence computation. Notice the clarity with which the fault patterns stand out, which would be difficult to decipher from the seismic alone. A chair display in Figure 1c shows the correlation of the fault patterns with their seismic signatures.

Curvature

Lisle (1994) demonstrated the correlation of a curvature measure (Gaussian) with open fractures measured on outcrops. Though the exact relationship between the open fractures, paleostructure and present-day stress is not yet clearly understood, different authors (Roberts (2001), Hart et al. (2002), Sigismondi and Soldo (2003), and Massafero et al. (2003)) have demonstrated the use of seismic measures of reflector curvature to map subtle features and predict fractures. A significant advancement in this direction has been the volumetric computation of curvature (Al-Dossary and Marfurt, 2006). By first estimating the volumetric reflector dip and azimuth that represents the best single dip for each sample in the volume, and followed by computation of curvature from adjacent measures of dip and azimuth, a full 3D volume of curvature values is produced. There are many curvature measures that can be computed, but the most-positive and most-negative curvature measures are the most useful in that they tend to be most easily related to geologic structures. An attractive feature of curvature computation is the ability to be able to perform multispectral analysis of curvature which depicts different features at different scales of analysis (Chopra and Marfurt, 2007).

Figure 2 shows a comparison of time slices at t = 2104 ms from (a) seismic, (b) coherence, and (c) most-positive curvature. Notice that while the coherence display is featureless in the high coherence (white) areas, the most-positive curvature display illuminates a series of N-S trending flexures.

Conclusions

Seismic attributes are very useful in the characterization of faults and fractures in 3D seismic data volumes. Dip-magnitude and dip-azimuth maps are useful in identifying subtle displacements that may not be seen on seismic amplitude data. Curvature attributes, being derivatives of

reflector dip and azimuth, further highlight these details, with modern implementations provide volumetric images at different wavelengths. Modified eigen decomposition coherence algorithms are designed *not* to be sensitive to dip; rather, they provide maps of lateral changes in waveform. Mathematically independent, coherence, and curvature images are often coupled through the underlying geology.

Acknowledgements

We thank Oilexco, Calgary, for the granting us permission to show the data examples included in this abstract. We also thank Arcis Corporation for the permission to publish and present this work.

References Cited

Al-Dossary, S., and K.J. Marfurt, 2006, Multispectral estimates of reflector curvature and rotation: Geophysics, v. 71, p. 41-51.

Bahorich, M.S., and S.L. Farmer, 1995, 3-D seismic discontinuity for faults and stratigraphic features: The coherence cube: The Leading Edge, v. 14, p. 1053-1058.

Chopra, S., 2002, Coherence cube and beyond: First Break, v. 20/1, p. 27-33.

Chopra, S., and K.J. Marfurt, 2007, Multispectral volumetric curvature adding value to 3D seismic data interpretation: CSPG/CSEG Convention, Calgary.

Gersztenkorn, A., and K.J. Marfurt, 1999, Eigen structure-based coherence computations as an aid to 3-D structural and stratigraphic mapping: Geophysics, v. 64, p. 1468-1479.

Hart, B.S., R.A. Pearson, and G.C. Rawling, 2002, 3-D seismic horizon-based approaches to fracture-swarm sweet spot definition in tight-gas reservoirs: The Leading Edge, v. 21, p. 28-35.

Lisle, R.J., 1994, Detection of zones of abnormal strains in structures using Gaussian curvature analysis: AAPG Bulletin, v. 78, p. 1811-1819.

Marfurt, K.J., R.L. Kirlin, S.L. Farmer, and M.S. Bahorich, 1998, 3-D seismic attributes using a semblance-based coherency algorithm: Geophysics, v. 63, p. 1150-1165.

Marfurt, K.J., V. Sudhaker, A. Gersztenkorn, K.D. Crawford, and S.E. Nissen, 1999, Coherency calculations in the presence of structural dip: Geophysics, v. 64, p. 104-111.

Masaferro, J.L., M. Bulnes, J. Poblet, and M. Casson, 2003, Kinematic evolution and fracture prediction of the Valle Morado structure inferred from 3-D seismic data, Salta Province, northwest Argentina: AAPG Bulletin, v. 87, p. 1083-1104.

Rijks, E.J.H., and J.C.E.M., Jauffred, 1991, Attribute extraction: An important application in any detailed 3-D interpretation study: The Leading Edge, v. 10, p. 11-19.

Roberts, A., 2001, Curvature attributes and their application to 3-D interpreted horizons: First Break, v. 19, p. 85-99.

Sigismondi, M., and J.C. Soldo, 2003, Curvature attributes and seismic interpretation: Case studies from Argentina basins: The Leading Edge, v. 22, p. 1122-1126.

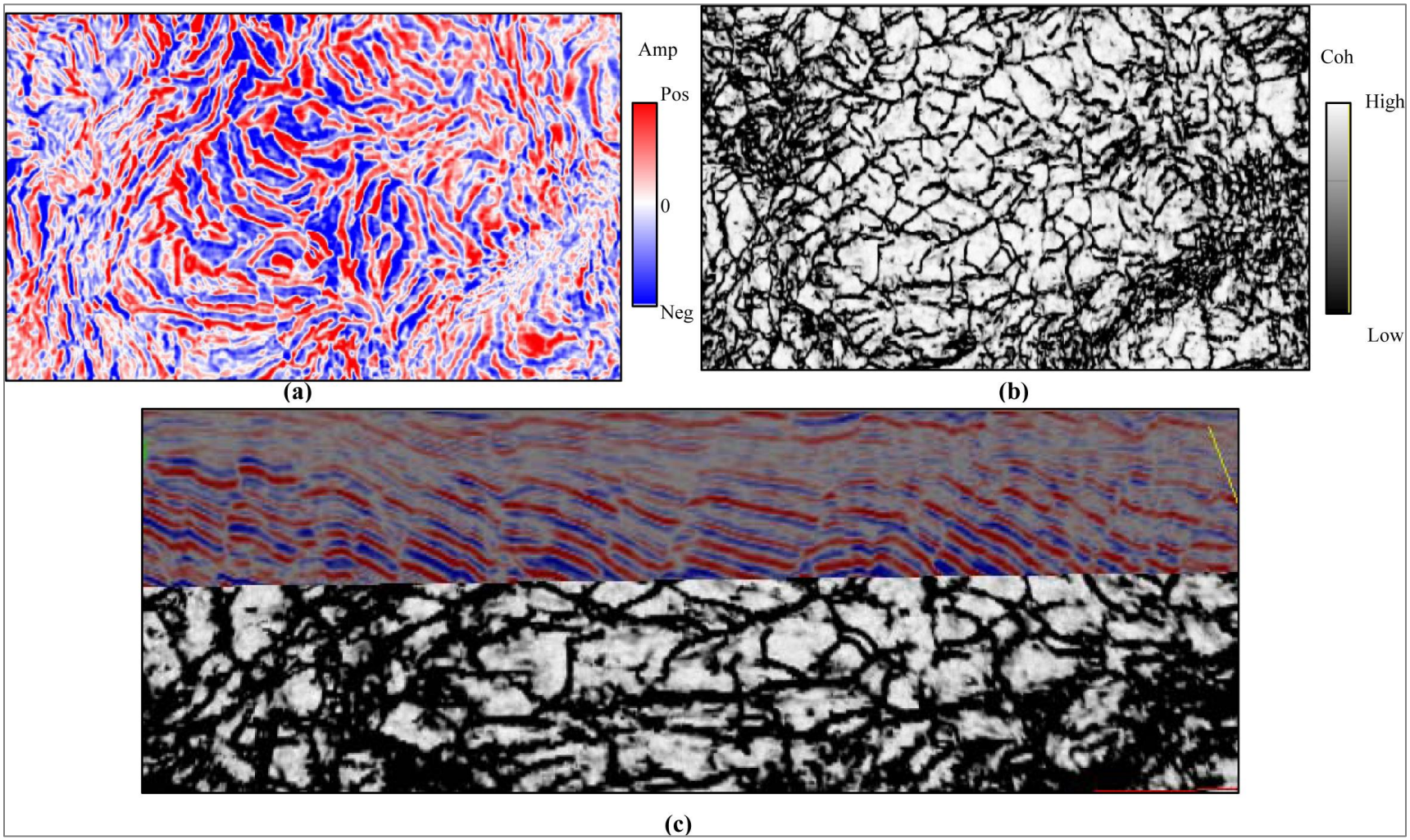

Figure 1. Time slice at 1240 ms through (a) a seismic volume from North Sea, (b) the equivalent coherence slice generated using a modified eigen decomposition algorithm with a robust dip-steering option. Notice the accurate imaging of the fault pattern seen on the coherence slice in (b), which is almost impossible to detect on the seismic. (c) Shows a chair display of the fault patterns on the coherence and a vertical seismic section. This helps correlate the fault breaks with their seismic signatures. (Data courtesy of Oilexco, Calgary)

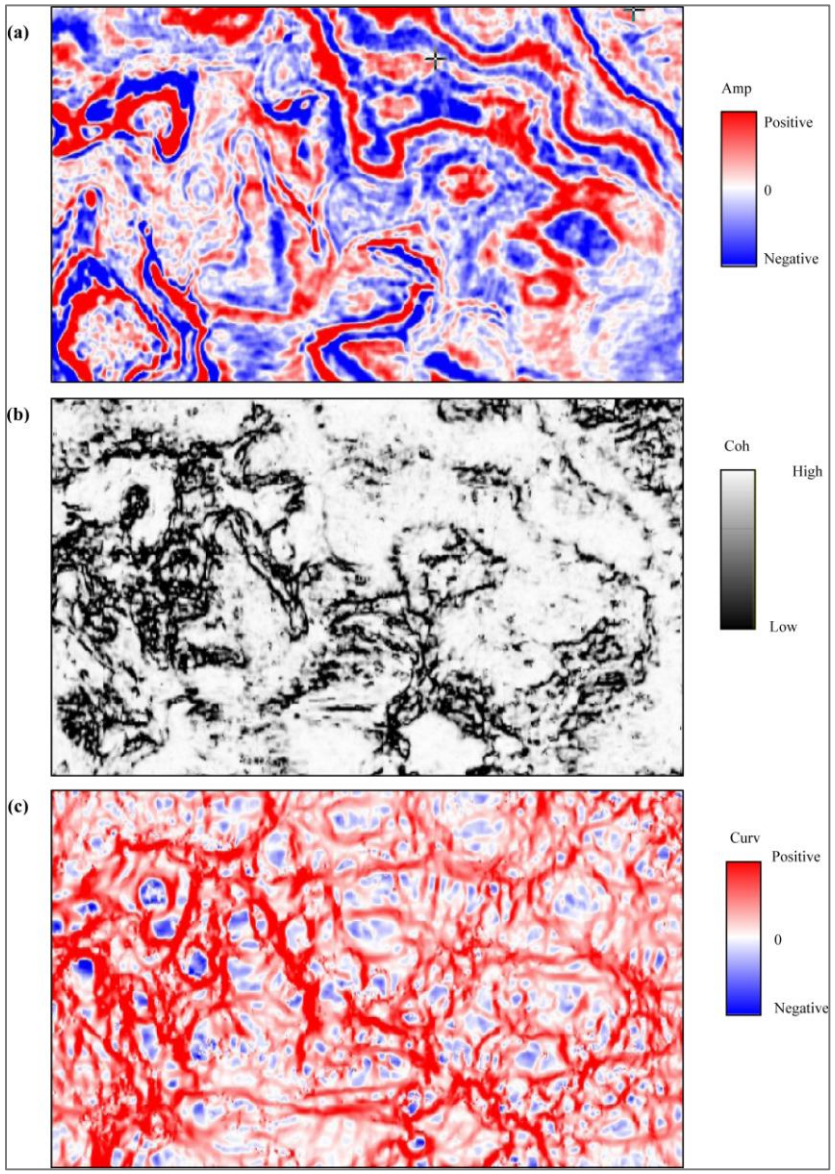

Figure 2. Time slice at 2104 ms through (a) seismic, (b) coherence, and (c) most-positive curvature volumes. Notice that while the coherence display is featureless in the high coherence (white) areas, most-positive curvature delineates N-S flexures in those areas. Also note the through-going E-W flexure in the southern part of the survey. (Data courtesy of Oilexco, Calgary).